SCITECH
RESEARCH ORGANISATION

Ebonex-Supported PtM Anode Catalysts for PEM Water Electrolysis

G. Borisov, A. Stoyanova, E. Lefterova, S. Vasilev, E. Slavcheva
Institute of Electrochemistry and Energy Systems – BAS, 10 G. Bonchev Str., BG-1113 Sofia.

Abstract

The work presents a research on the preparation of Pt-based bimetallic catalysts dispersed on commercial Magnelli phase titania (Ebonex[@]) by sol gel method and investigation of their activity toward the oxygen evolution reaction (OER) in polymer electrolyte membrane water electrolysis (PEMWE). The catalytic support is also used for preparation of a carbon-free gas diffusion layer (ET30) integrated in the oxygen electrode of the membrane electrode assembly (MEA). The performance characteristics of MEA with PtM/Ebonex on ET30 are investigated in a laboratory PEMWE and compared to those of MEA with commercial carbon-based GDL with the same anode catalyst. It is proven that the chemical nature and electron density of the second metal have an essential effect on the catalyst surface structure and properties, including the lattice parameter, particle size, and electronic surface state state which in turn, reflect on the electrochemical behavior and catalytic activity. The catalysts PtCr/Ebonex and PtMn/Ebonex having deficiency of electrons in the valent d-orbital do not form an alloy with Pt and have lower catalytic activity. In contrast, the metallic components in PtFe/Ebonex and PtCo/Ebonex form a solid solution which results in changes in the catalyst structure and surface electron state, leading to enhanced OER efficieny compared to pure Pt/Ebonex.

Keywords: Polymer Electrolyte Membrane Water Electrolysis; Pt-Based Bimetallic Catalysts; Magnelli Phase Titania; Oxygen Evolution Reaction; Carbon-Free Gas Diffusion Layer.

1. Introduction

The polymer electrolyte membrane water electrolysis (PEMWE) is the clearest and simplest method for generation of hydrogen with high purity. The technology is compatible with the renewable energy sources and is gaining increasing interest for practical applications. The design and nominal capacity of PEMWE can vary in broad ranges depending on the needs of the end user. At the same time the main active element where the energy conversion (electrical to chemical) takes place, the membrane electrode assembly (MEA), has nearly unchangeable structure and can be adapted to any specific requirements [1-3]. The MEA properties determine the PEMWE performance and reflect essentially on the cost of the produced hydrogen. To ensure high efficiency, the electrodes integrated in the MEA should have excellent electrical conductivity, highly developed surface, and active elecrocatalysts capable to work long hours at aggressive conditions (high electrode potentials, low pH, high humidity, etc.). The partial electrode reaction of hydrogen evolution (HER) has fast kinetics and on proper catalysts such as Pt it proceeds at very low overvoltages close to the thermodynamic potentential. In contrast, the oxygen evolution reaction (OER) is much more problematic. It not only proceeds at high overvoltages due to the slow kinetics but the presence of highly aggressive oxygen radicals at elevated temperatures and humid atmosphere cause corrosion of the catalyst and/or the catalytic substrate followed by gradual degradation of the anode [4-6]. Therefore, the choice of the OER catalyst is of key importance for the efficiency and durability of the whole system. It is well known that the catalytic activity depends on variety of factors such as the catalyst chemical nature, electronic surface state, particle size, presence of impurities etc. which affect the formation and strength of the intermediate chemical bonds and determine the mechanism and rate of the corresponding electrode reactions [7-10]. The catalytic support should offer highly developed surface combined with excellent electronic conductivity. The anode catalyst supports should also have an enhanced corrosion resistance in order to withstand the aggressive environment at the oxygen electrode. The most widely used carbon supports oxidize at high anodic potentials where oxygen evolution takes place which excludes their application in water electrolysis. For these reasons in the last

years there is an intensive search of novel corrosion resistant supporting materials. Some conductive ceramics (metal carbides, nitrides, and oxides) are considered as promising alternative of the carbon supports [11-16]. In this respect the Magnelli phase titania known under the registered trade name Ebonex (Atraverda, Inc., UK) is a subject of particular interest. Ebonex is a nonstoichiometric mixture of titanium oxides with general formula Ti_nO_{2n-1}, where $4 \leq n \leq 10$. This material has a unique combination of electrical conductivity approaching that of a metal ($\approx 1.10^3\ \Omega^{-1}.cm^{-1}$) and high corrosion resistance both in acid and in basic solutions [17,18]. Its chemical composition and hypo-d-electron character suggest an ability to interact with hyper-d-electron metals such as Pt, Ni, Co, etc., which is a prerequisite for synergism and increase of catalytic activity [13, 14]. This work presents a research on the preparation of Pt-based bimetallic catalysts, dispersed on Ebonex by sol gel method and investigation of their activity toward the OER in PEMWE. The Ebonex is also used for preparation of carbon-free gas diffusion layer ET30 integrated in the MEA oxygen electrode.

2. Experimental

The choice of the syntesyzed catalytic compositions PtM (M = Cr, Mn, Fe, Co) is based on their chemical nature, electronic state, and analysis of the available literature data in view of the possibility by partial replacement of Pt with cheaper transition metals to realize hyper-hypo-d-electron effect leading to synergism and enhanced catalytic efficiency [8, 9, 19]. The synthesis of the chosen composite materials consists in direct selective grafting of the metals from acetilacetonate precursors $M((C_5H_7O_2)n)_m$ or M-acac on Ebonex® (Atraverda, UK), following a previously described procedure [20]. Before synthesis, the as-obtained supporting material (particle size 5 µm) is pre-treated in ball mill for 40h to reduce the size and thus, to increase the surface area of the support. The metal part of the obtained composite PtM/Ebonex catalysts is 20 wt.% and the Pt:M ratio is 1:1.

The catalysts chemical composition, structure, morphology and surface state are studied using variety of methods for bulk and surface analysis. The surface structure and morphology are investigated by scanning electron microscopy (SEM) using a ZEISS GEMINI 982 microscope with an acceleration voltage of 3 kV and a magnification up to 200 000. The chemical composition of the catalysts is examined by energy-dispersive X-ray spectroscopy (EDX) as a part of the scanning electron microscope appliance. The crystal structure and phase identification are analysed by method of X-ray diffraction (XRD), using diffractometer Philips APD15. The diffraction data are collected at a constant rate $0.02^o\,s^{-1}$ over an angle range of $2\theta = 10-90^o$. The size of crystallites is determined by Scherrer equation [21]:

$$d = k\lambda/\beta cos\theta \qquad (1)$$

where d is the average dimension of crystallites, k is the Scherrer constant; l is the X-ray wavelength; θ is the Bragg angle and β is the peak broadening in radians.

The XPS analysis is performed with an ESCALAB MK II (VG Scientific, England) electron spectrometer. The photoelectrons are excited with a twin anode X-ray source using Al Kα ($h\nu$ = 1486.6 eV) radiation. C1s photoelectron line at 284.8 eV is used as a reference for calibration. Curve fitting of the core-level XPS lines is carried out using CasaXPS software with a Gaussian-Lorentzian product function and a non-linear Shirley background.

The catalysts are integreated in MEA (working area 0.5 cm^{-2}) consisting of: working electrode (anode) with catalytic layer (0.2 mg PtM/Ebonex cm^{-2}) spread on a commercial carbon-based GDL (Toray paper, Alfa Asear) or on a laboratory prepared carbon-free GDL (ET 30) containing a mixture of Ebonex and polythetrafluorethylene; proton conductive membrane Nafion® 117 (180 µm); counter electrode (0.4 mgPt cm^{-2}, BASF). The assembling conditions and MEA fabrication steps are presented in details elswhere [22]. The catalytic efficiency of the syntesized PtM/Ebonex toward the oxygen evolution and the MEA performance characteristics are investigated in a laboratory PEMWE (single cell) applying the common electrochemical techniques of cyclic voltammetry, potentiodynamic, and potentiostatic polarization. The measurements are carried out using electrochemical equipment POS 2, Bank Elektronik.

3. Results and Discussion

3. 2. Physical Characterization

Monometallic Pt/ Ebonex Catalyst

In order to distinguish the influence of the second metal and the interactive support on the physical properties and catalytic activity of the composite PtM/Ebonex catalysts, first the monometallic Pt/Ebonex is prepared and investigated. The SEM images presented in fig. 1 show that platinum is homogeneously dispersed on the substrate, while the Pt clusters differ in size. The observed partial agglomeration is not typical for carbon-supported platinum in which case it occurs after long service. A possible reason beside the different chemical nature is the size of the Ebonex particles. Although after the applied ball mill pre-treatment it is essentially reduced (from 5 µm to 60- 100 nm), the overall specific surface is still much lower compared to that of the most often used carbon supports (45-50 m^2 g^{-1} vs. 240 m^2 g^{-1} for Vulcan XC72, for instance [23]).

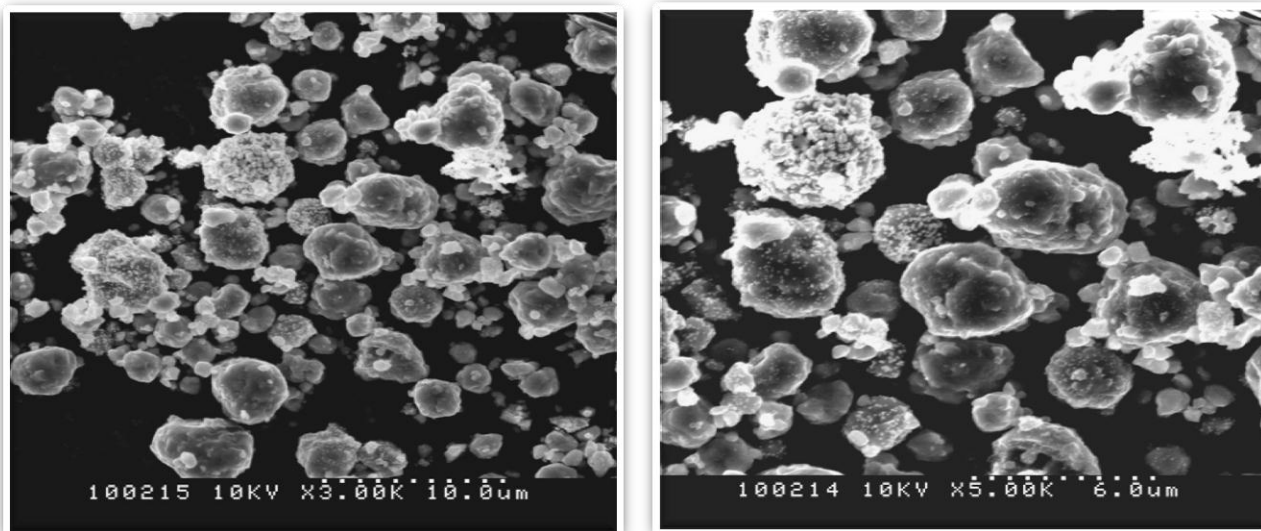**Fig. 1: SEM Images of Catalyst Pt/Ebonex at Different Magnification**

Fig. 2: XRD Spectra of the Support and the Monometallic Pt/Ebonex Catalyst
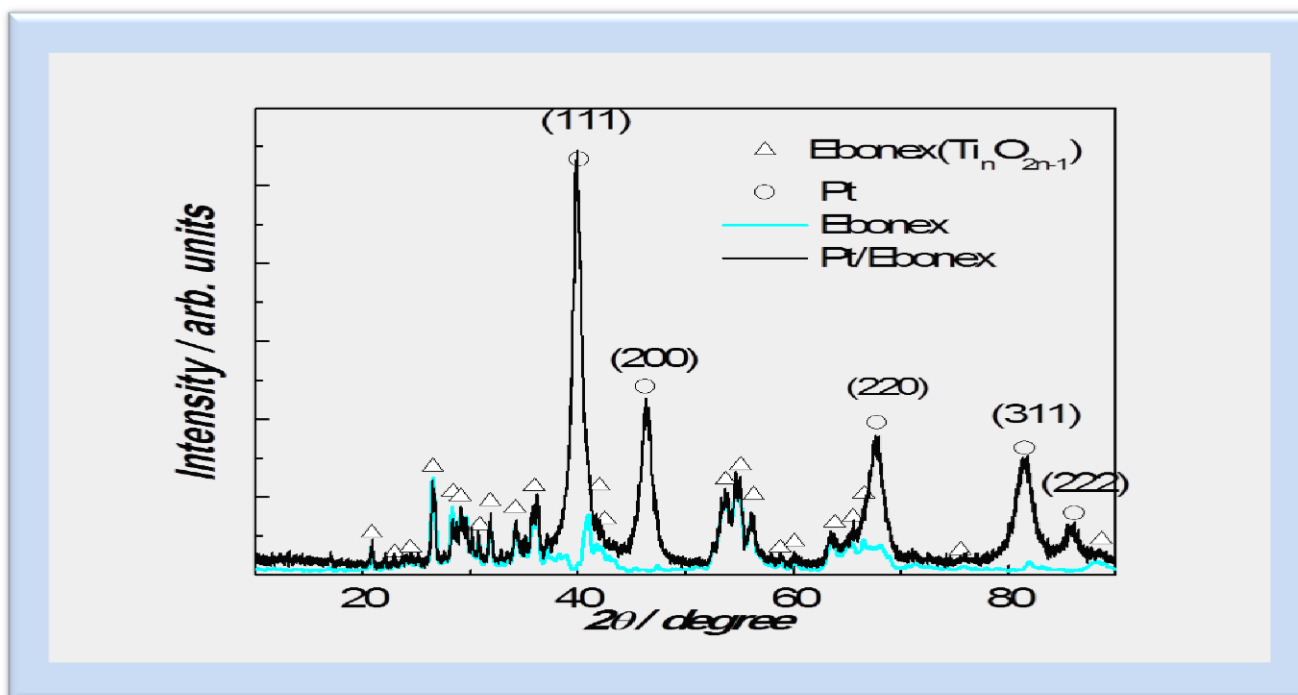

Fig. 2 presents the XRD spectra of Pt/Ebonex. The position of platinum peaks testifies that Pt is in a polycrystalline metallic form. The predominant crystallite orientation is in direction Pt(111) however, the peaks corresponding to Pt(200), Pt(220), and Pt(311) crystallographic planes are also well recognized. The size of Pt crystallites determined by Scherer equation using the FWHM of Pt(111) peak is in the range 6-7 nm. The specific surface area of the catalyst, determined by BET analysis is around 47 $m^2 g^{-1}$. XPS spectra presented in fig. 3 confirm that Pt is mainly in metallic form but traces of surface Pt^{4+} и Pt^{2+} are also registered. The binding energy is slightly shifted in positive direction compared to unsupported Pt, suggesting electronic interactions with the oxide *hypo-d-electron* support.

Fig. 3: XPS Pt 4f Spectra of Pt/Ebonex
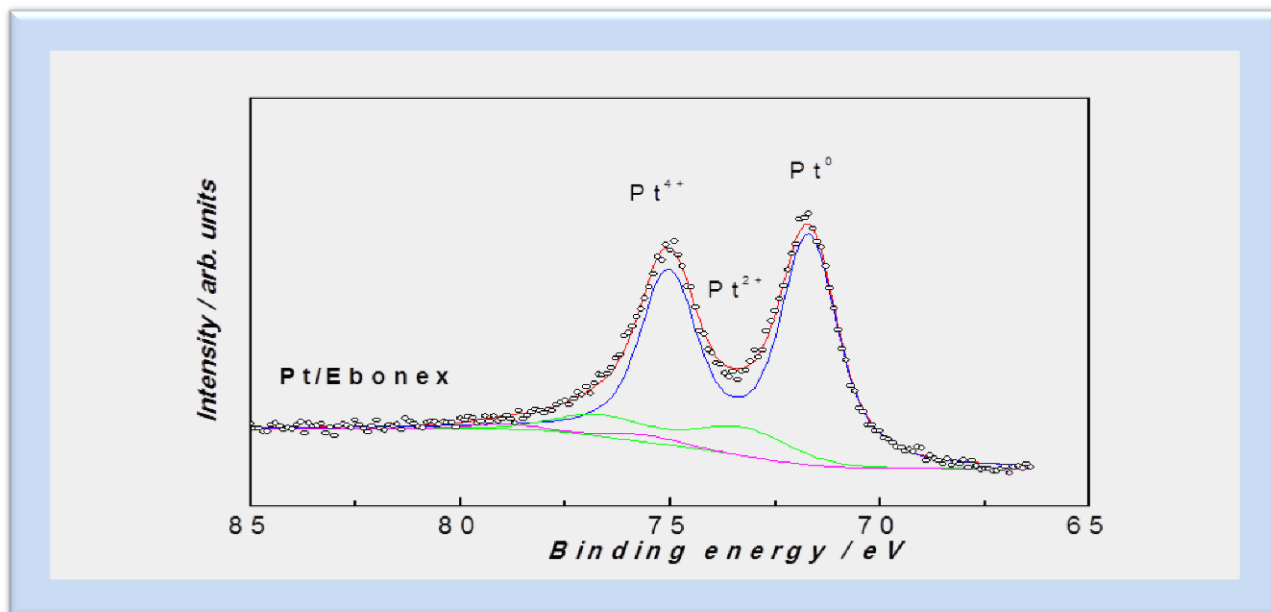
Bimetallic PtM/Ebonex catalysts

The analysis of the spectroscopic data obtained for the synthesized bimetallic catalysts shows that depending on the established type of interaction between both metallic components.they can be divided in two groups: PtCr/Ebonex, PtMn/Ebonex and PtFe/Ebonex, PtCo/Ebonex.

Fig.4 presents XRD spectra of the catalysts from the first group. The patterns show only the characteristic peaks of Pt and Ebonex, meaning that the second metal is in amorphous, most probably oxidized state. The observed lines of MnO in the spectrum of PtMn/Ebonex have very low intensity which supports this assumption.

Fig. 4: XRD Spectra of Ebonex, Pt/Ebonex, PtMn/Ebonex и PtCr/Ebonex
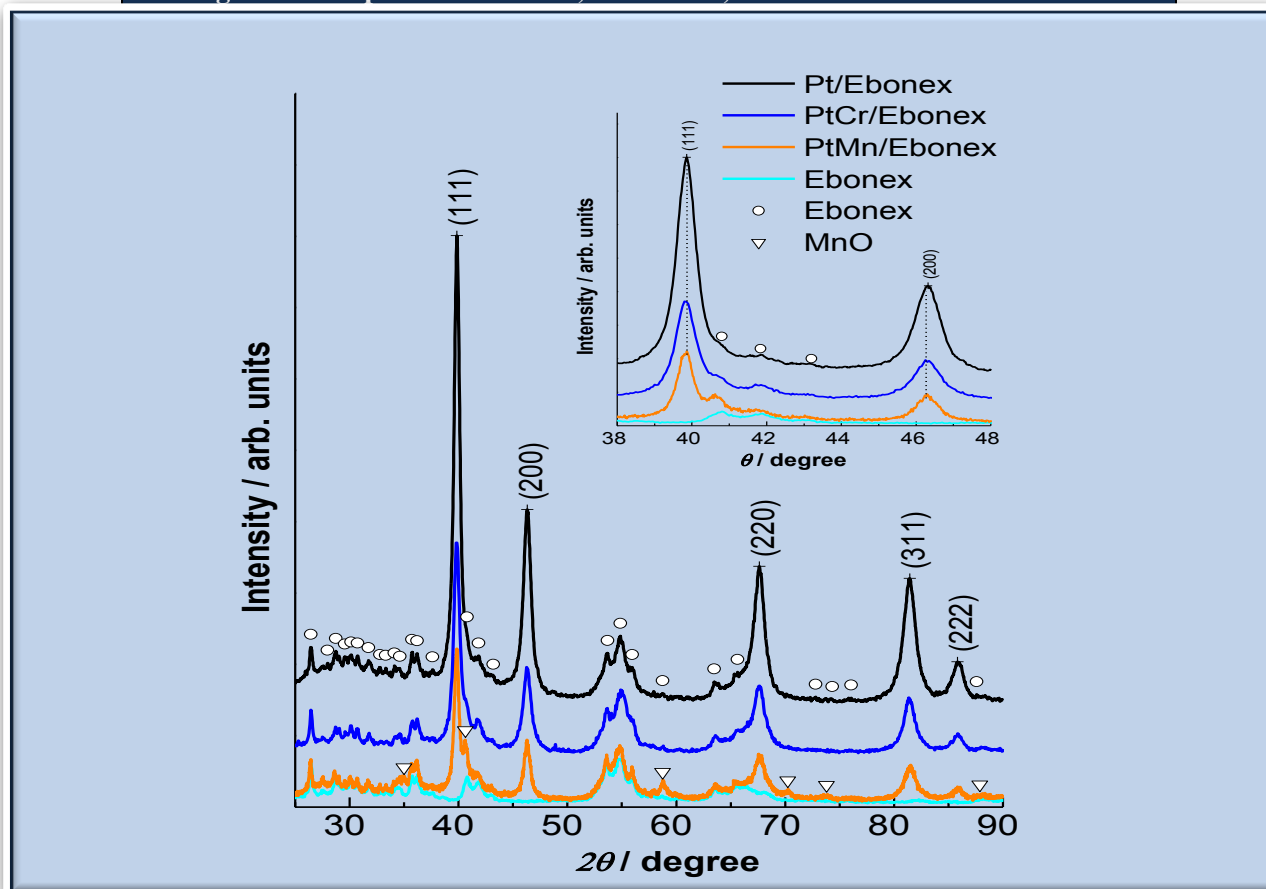
The position of Pt peaks does not change in presence of the second metal. At the same time their intensity in the spectrum of Pt/Ebonex is much higher compared to the bimetallic systems, which is in accordance with the decreasedplatinum content.

The calculated values of Pt lattice parameter, *a*, and the size of Pt crystallites, *d*, for all synthesized catalysts are summarized in Table 1. For the first group catalysts *a* and *d* do not differ essentially and are very close to the pure platinum parameters, meaning that Cr and Mn are not incorporated in the Pt lattice.

| **Tabele 1: Pt Cell Parameter and Crystal Size of the Synthesized Mono and Bimetallic Catalysts**			
Catalyst	**Size of Pt Lattice Parameter a [Å]**	**Size of the Pt Crystallites d [nm]**	
		(111)	(200)
Pt/Ebonex	3.9195	14	12
PtCr/Ebonex	3.9204	12	10
PtMn/ Ebonex	3.9186	16	13
PtFe/Ebonex	3.7690	6	6
PtCo/Ebonex	3.7470	4	5

The XPS spectra presented in fig. 5 confirm the results from the XRD analysis.Pt is predominantly in metallic state as small amounts of oxidized platinum atoms are registered on the surface, better distinguished for PtCr/Ebonex (fig. 5a). Both non-noble transition metals are in an oxidized state (figs. 5b, 5c).

Fig. 5: XPS Spectra of Pt/Ebonex, PtMn/Ebonex, PtCr/Ebonex; a) Pt4f; (b) Mn2p; c). Cr2p
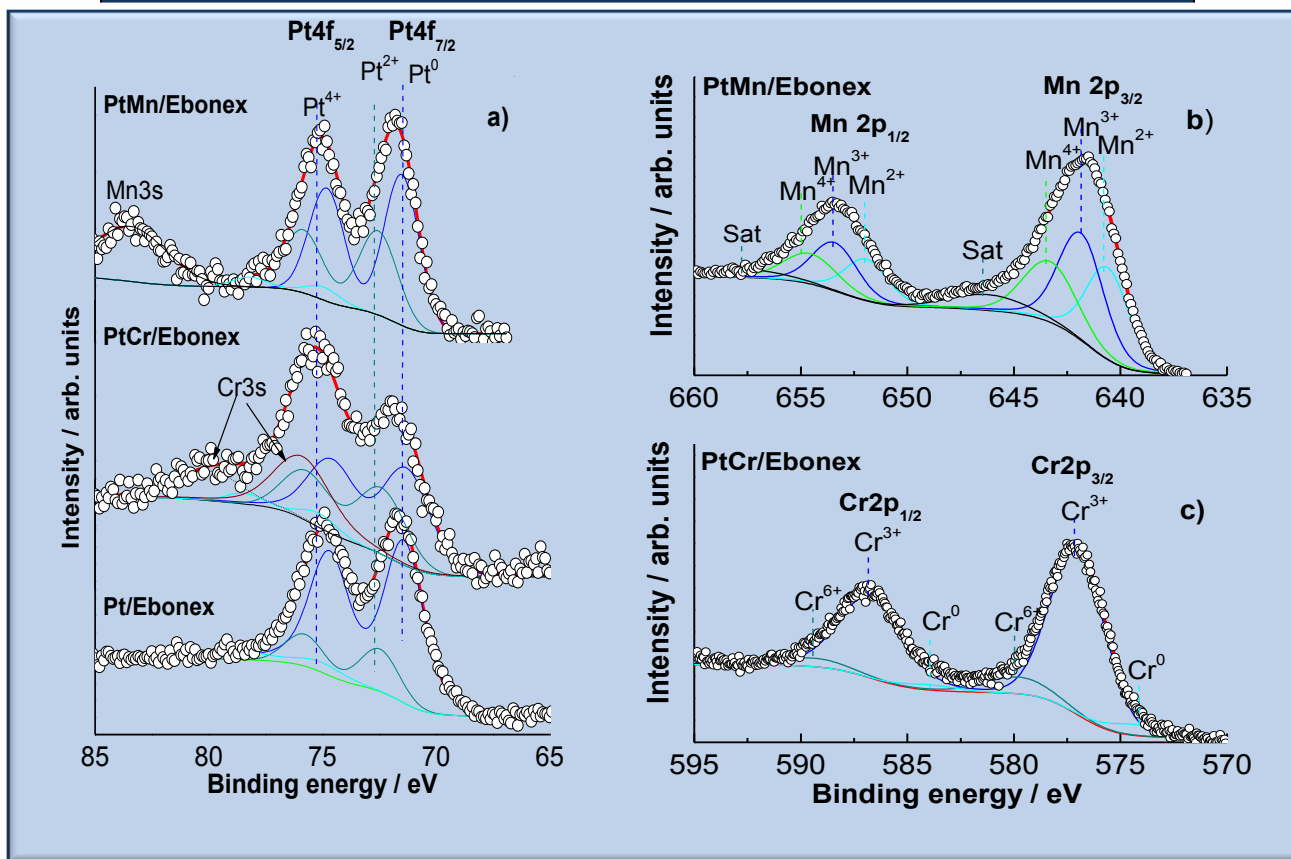
The results from XRD analysis of the second group catalysts are presented in fig. 6 (a, b) where the spectra of the support and the corresponding monometallic compositions (Pt/Ebonex, Fe/Ebonex, Co/Ebonex) are also included for comparison.

Fig. 6: XRD Spectra of PtFe/Ebonex (a) and PtCo/Ebonex (b) Compared with the Corresponding Monometallic Compositions
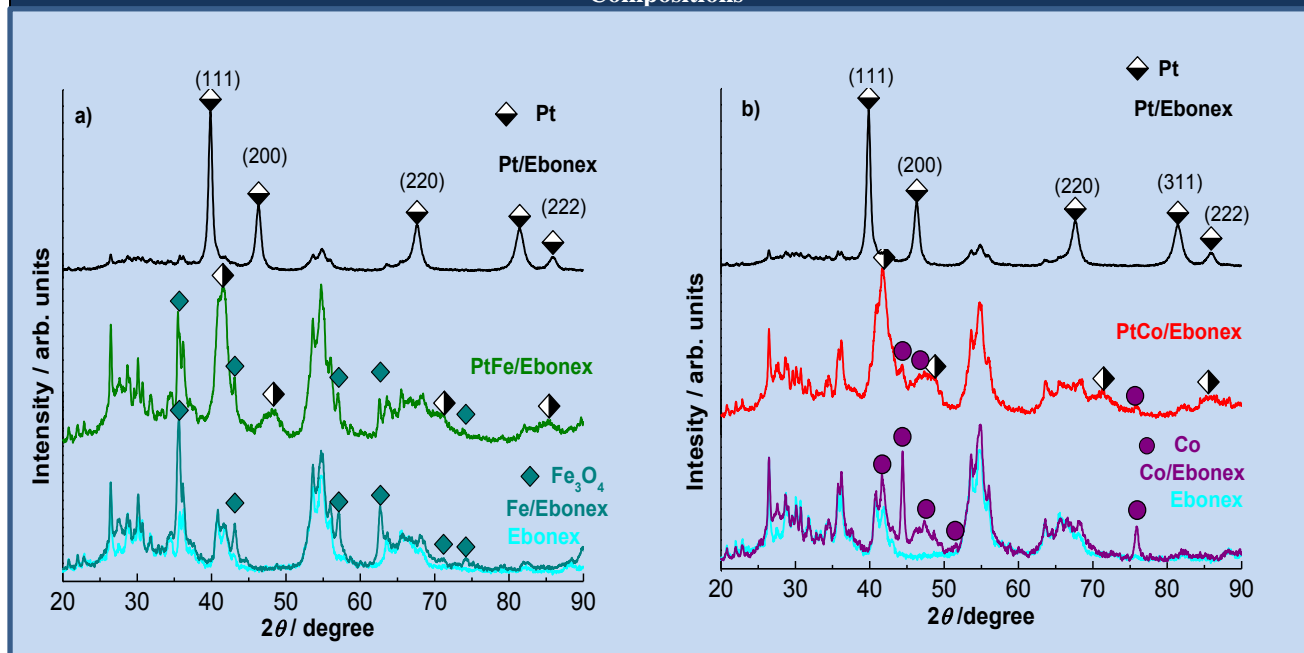
In similarity with the first group catalysts, the peaks of Pt and the support are clearly seen in XRD patterns of all compositions. The spectrum of PtFe/Ebonex registers presence of Fe_3O_4 oxide phase, while for PtCo/Ebonex only traces of metallic Co are found. The platinum peaks in the spectra of the bimetallic catalysts are essentially shifted to higher diffraction angles, implying changes in the structure and/or the size of Pt particles. This is confirmed by the calculated values of Pt crystal lattice parameter, *a,* and the size of the crystallites, *d* (Table 1). The cell parameter for PtFe/Ebonex and PtCo/Ebonex decreases essentially compared to Pt/Ebonex. The analysis of XRD data suggests that most of the second metal atoms are incorporated in the platinum lattice, causing its shrinkage and formation of solid solution with Pt.

It is well known that the alloying of Pt with other metals leads to changes in the electronic state of platinum valent shell and a corresponding displacement of the surface binding energy which can be registered by XPS analysis [24, 25]. In fig. 7 (a-d) are shown the results obtained for Pt 4f, Fe2p, Co2p, and O1s XPS spectra of Pt/Ebonex, PtFe/Ebonex and PtCo/Ebonex.
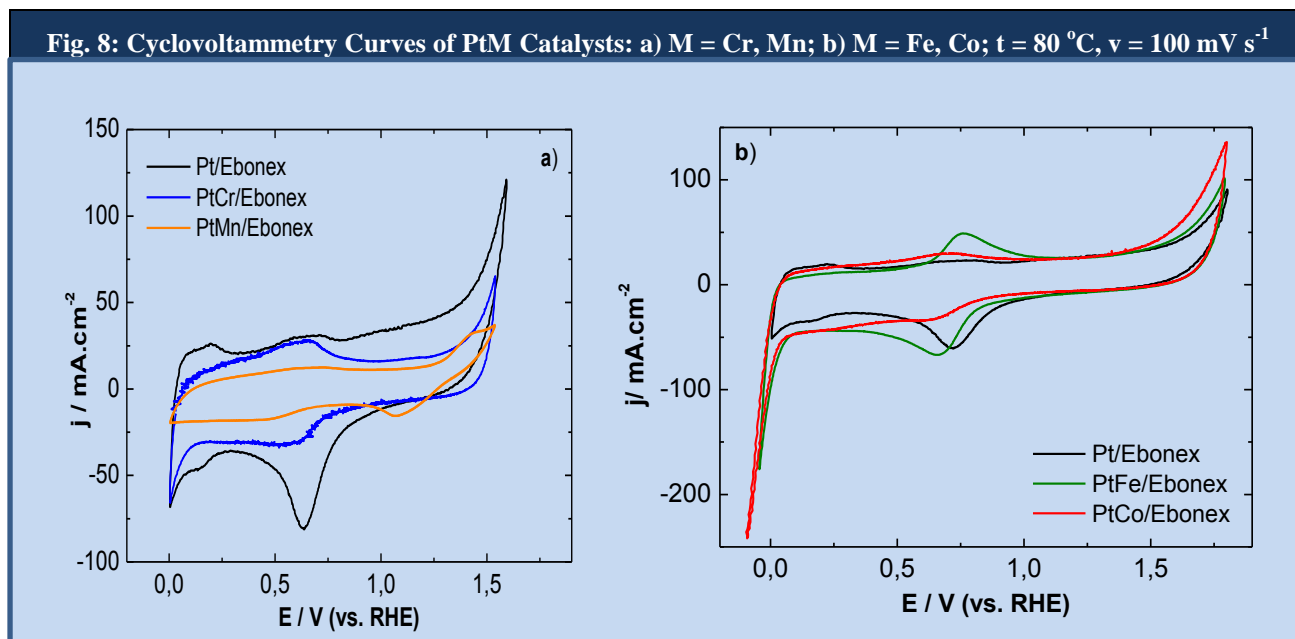

Fig. 7: XPS Spectra of the Catalysts From the Second Group: a) Pt 4f; b) Fe2p; c) Co2p; d) O1s
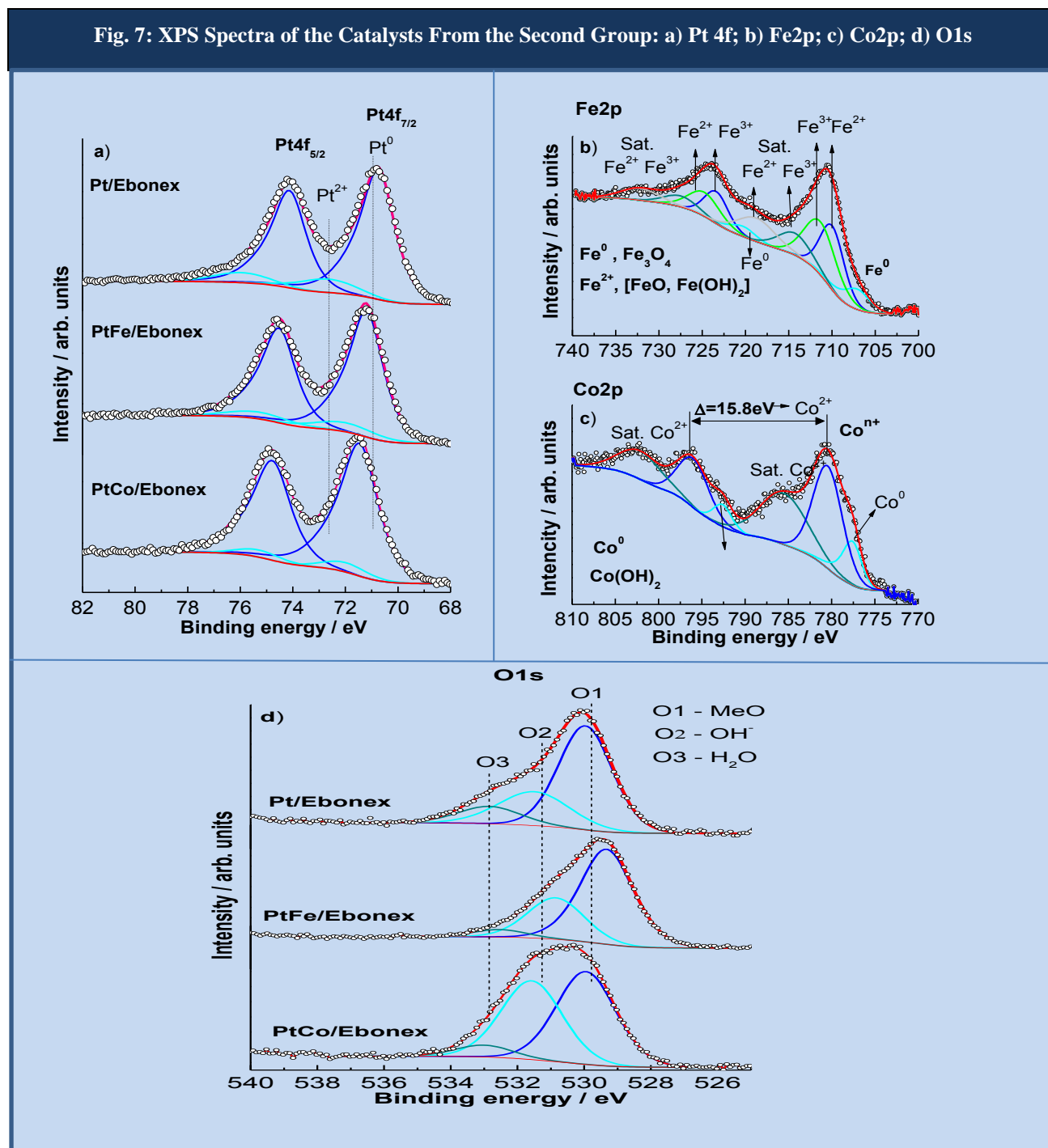
The data are in accordance with the results from XRD, showing that Pt presents mainly in metallic form as traces of of OH groups are also registered on thesurface (fig. 7a). The binding energy of Pt4f electrons for the bimetallic systems is shifted in positive direction relative to Pt/Ebonex, which is another proof for the already discussed alloying with Fe and Co. In contrast to Pt, Fe and Co present both in metallic and in oxidized form on the catalyst surface (fig. 7b,c). The performed deconvolution of Fe2p XPS spectrum registers Fe^{2+}, Fe^{3+} и Fe^{o}. The satellite structure as well as the orbital spin-splitting in Co2p spectrum is characteristic for $Co(OH)_2$ which is confirmed by the O1s spectra (fig. 7d). As it is seen, the signal corresponding to OH presence is strongest in O1s spectrum of PtCo/Ebonex.

3.3. Electrochemical Characterisation

To investigate the efficiency of the synthesized catalysts they are integrated in the anode of MEA with a polymer membrane electrolyte Nafion 117. To obtain qualitative information about the electrochemical activity and the nature of the processes occurring on the catalyst surface, cyclovoltammetry tests are performed (fig. 8a, b).

Fig. 8: Cyclovoltammetry Curves of PtM Catalysts: a) M = Cr, Mn; b) M = Fe, Co; t = 80 ^{o}C, v = 100 mV s^{-1}

The CV curve of Pt/Ebonex shows typical behaviour regarding both the hydrogen and the oxygen potential regions, while the CVs of the bimetallic systems are rather different. The curves of PtMn/Ebonex and PtCr/Ebonex (fig. 8a) have rather featureless profile. The current peaks in the hydrogen region are missing and the hydrogen evolution is suppressed which can be explained with the presence of metal oxides registered by XDR and XPS analysis. The broad shoulder on the PtCr/Ebonex CV in the potential range 0.3-0.4 V is related to gradual changes in valent state of Cr, while PtMn/Ebonex shows a typical capacitive behavior in a very broad potential range - up to 1.3 V. For both bimetallic catalysts the oxygen evolution reaction starts at more positive potentials (1.55 V and 1.6 V for PtCr/Ebonex and PtMn/Ebonex, respectively) and proceed slower compared to the monometallic Pt/Ebonex.

The cyclic voltammograms of the second group catalysts (fig. 8b) have similar area under the curves, suggesting that these catalysts possess comparable electrochemically active surface area. On the CV of PtFe/Ebonex a reversible current peak appears at 0.70-0.75 which is related to changes in the valent state of Fe (Fe^{2+}/Fe^{3+}). The oxygen evolution reaction starts earlier on the bimetallic catalysts, indicting higher catalytic eefficiency comared to Pt/Ebonex.

The careful observation of the CV curves in fig. 8 shows that during the anodic potential scan there is more or less clearly depicted current peak in the range 0.70-0.75 V. According the literature such peak is often observed on the CV of various carbon supported catalysts and is prescribed to oxidation of the support [26]. Since in our case the catalysts are deposited on Ebonex, the appearance of this peak might be prescribed to oxidation of the carbon GDL, leading to gradual degradation of the anode with time. To verify this assumption, accelerated stability tests are performed. The procedure includes long term potential cycling in the water window range, accompanied by periodic interruption of the applied voltage and recording of the CV after defined number of "work-relaxation" cycles. The number of the potential scans in each working cycle is 100 and the relaxation time is 30 minutes.

Fig. 9a presents the cyclovoltammetry curves of MEA with anode catalyst Pt/Ebonex after 10 and 100 "work-relaxation" cycles. The observed shrinkage of the CV is due to degradation of GDL leading to loss of adhesion with the catalytic layer and thus, to loss of active surface.

To avoid the observed degradation of the MEA performance due to corrosion of the anode, a carbon-free GDL based on Ebonex (ET30) is developed and optimize in regard to electrical conductivity and porosity as reported elsewhere [22]. Fig. 9b shows the results from the accelerated stability tests of Pt/Ebonex catalyst dispersed on laboratory prepared non carnon GDL ET30. The observed current peaks on Pt/Ebonex curves in the hydrogen and oxygen potential ranges are much clearly depicted compared to those of the same catalyst deposited on the commercial carbon GDL. The conture of the CVs and the width of the peaks do not change with cycling and are characteristic for polycrystalline Pt with prevailing (111) orientation and low electrode porosity. The former is proven by the performed XRD analysis, while the latter can be explained with formation of comparatively dense structure of ET30 during the applied sintering of this non-carbon GDL [22]. At the same time the anodic peak at 0.75 V on fig. 9a prescribed to oxidation of carbon in the commercial GDL is not registered. The results obtained for the bimetallic PtFe/Ebonex and PtCo/Ebonex were similar - better depicted narrower current peaks and lower area of the CVs compared to those of the same catalysts on carbon GDL.

Fig. 9: Accelerated Cyclovoltammetry Tests of MEA with Pt/Ebonex anode deposited on carbon (a) and Non-Carbon (b) GDL after various "Work-Relaxation" Cycles; t = 80 ^{o}C, v = 100 mV s^{-1}
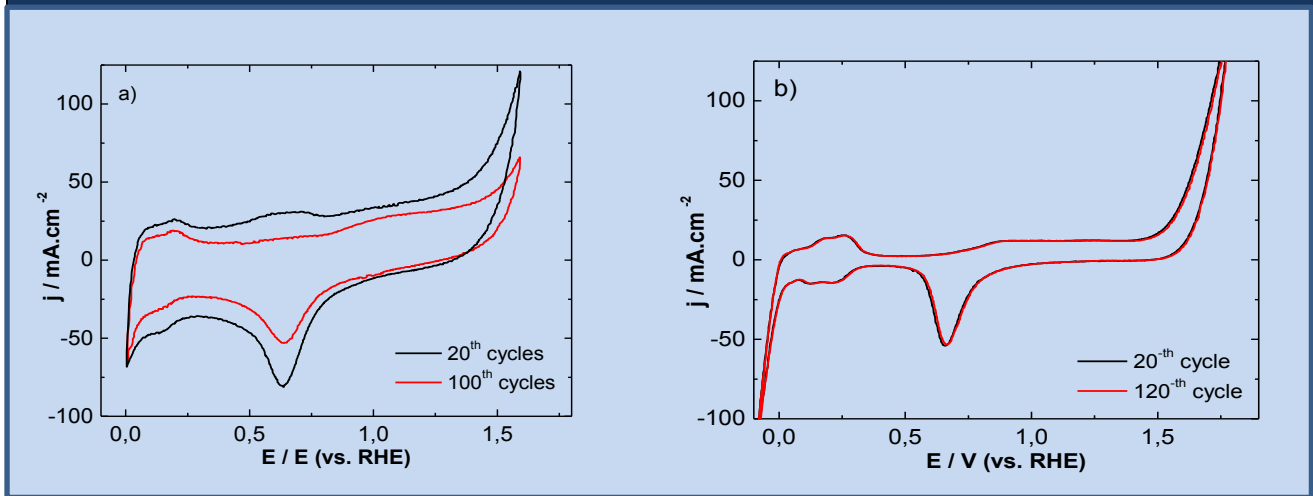
In fig. 10a are compared the anodic polarization curves of the second group PtM/Enonex catalysts on ET30, while fig. 10b presents the corresponding Tafel plots in mass activity

Fig. 10: Anodic Polarization Curves of MEA with PtM/Ebonex Catalyst (M = Fe, Co) on GDL ET30; v = 1 mV s^{-1}; t= 80 ^{o}C;a) E/j plots; b) Mass Activity in Tafel Plots, E/lgj$_m$
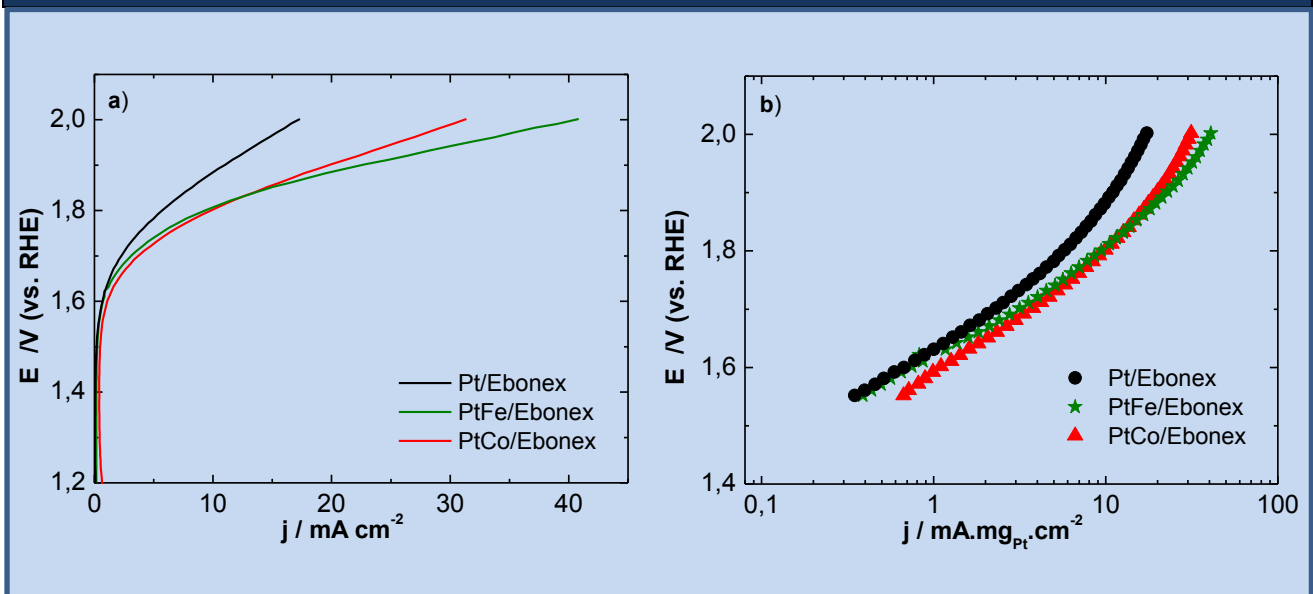
The results obtained show that the anodic reaction of oxygen evolution proceeds faster on the bimetallic catalysts as the process is most intensive on PtFe/Ebonex. For this catalyst the linear Tafel plot is longer and the slope of the curve

smaller, indicating highest catalytic efficiency. On the other hand, the measured current densities are lower compared to the same catalysts deposited on carbon GDL reported previously [20] This is in accordance with the assumption about the lower active surface area based on the CV data and implies lower catalyst utilization. The latter is confirmed by the calculated values of the catalysts morphology factor, *f,* which according the well known experimental method of da Silva is a measure for the not used part of the ctalysts [27]. The calculated data of the morphology factor and the corresponding catalysts utilization for the catalysts from the seconf group are summarized in Table 2. In accordance with the results obtained from the CV and polarization tests, the calculated values show about 2 times lower utilization when the catalyst layer is supported on the Ebonex-based GDL ET30.

Table 2: Morphology Factor (f) and Utilization (σ) of the Catalysts PtM/Ebonex (M = Fe, Co) on ET30 and Commercial Carbon GDL				
Catalyst	**Morphology Factor, *f***		**Catalytic Utilization, σ [%]**	
	ET 30	**C-GDL**	**ET 30**	**C-GDL**
Pt/Ebonex	0.73	0.38	27%	62%
PtFe/Ebonex	0.71	0.31	29%	69%
PtCo/Ebonex	0.59	0.33	41%	67%
*the data are taken from [20]				

Fig. 11 presents the results from long term potentiostatic experiments performed at 80 ^{o}C at intensive oxygen evolution (cell voltage 2V). The registered current densities reach stable values in the first hour and do not change further during the performed 240 h experiment. The results in figs. 9b and 11 show clearly a complete lack of degradation and confirm the stability of the prepared non-carbon GDL at the aggressive conditions of intensive oxygen evolution. The order of the increasing catalytic efficiency does not change, while the measured current densities are lower compared to MEA with commercial carbon-based GDL which is due to the insufficient specific surface of Ebonex and the lower porosity of the ET30, hindering the transport of the reagents to/from the MEA reaction zone.

The results from the performed potentiostatic tests are used to evaluate the efficiency of the electrolysis. The calculated data are summarized in Table 3 where:

l – platinum loading in [mg$_{Pt}$ cm^{-2}]

I – average current density at 1.8 V in [mA]

V^r_H – the measured volume of the produced hydrogen in [ml h^{-1}]

η_E – energy efficiency in [%]

V^t_H – the calculated theoretical hydrogen volume in [ml h^{-1}]

η_F – faradaic efficiency of the electrolysis in [%]

P – consumed energy in [Wh l^{-1}]

Fig. 11: Potentiostatic Polarization Curves of MEA with Anode Catalyst PtM/Ebonex (M = Co, Fe) and GDL ET30; U$_{cell}$ = 2 V, t = 80 ^{o}C
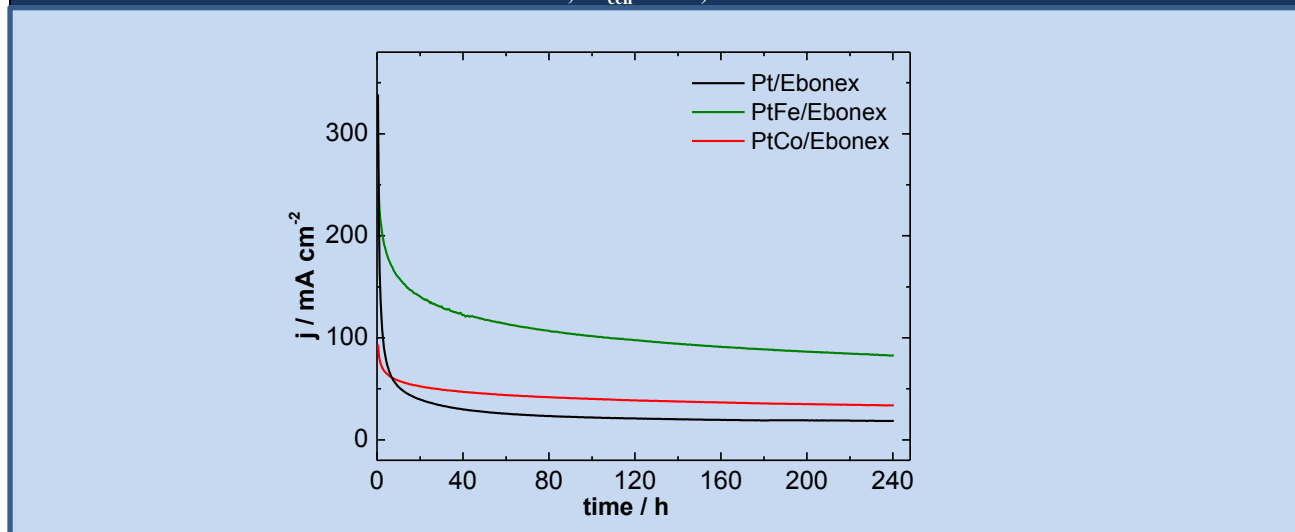
Table 3: Quantitative Data Assessing the Efficiency of the Electrolysis Using MEA with the Synthesized Anode Catalysts PtM/Ebonex (M=Co, Fe) and the Developed Non-Carbon GDL ET30							
Catalyst	**L** $[mg_{Pt} \, cm^{-2}]$	**I** [mA]	V^r_H $[ml \, h^{-1}]$	η_E [%]	V^t_H $[ml \, h^{-1}]$	η_F [%]	**P** $[Wh \, l^{-1}]$
Pt/Ebonex	0.2	18	6.5	63.9	9.7	67.3	5.54
PtCo/Ebonex	0.1	38	17.0	77.5	20.5	82.9	4.47
PtFe/Ebonex	0.1	96	47.0	86.7	52.0	90.4	4.08
the cathode is a commercial electrode with carbon-supported Pt and carbon-based GDL; working area 0.5 cm²							

The obtained quantitative data prove that the partial replacement of Pt with the chosen non-noble metals results in increased efficiency of the PEM water electrolysis. The energy required for generation of a liter hydrogen decreases with 20% and 29% for PtCo/Ebonex and PtFe/Ebonex, respectively at twice lower content of the noble metal loading. The reaction of oxygen evolution which is the main source of energy losses is facilitated as the effect is strongest for PtFe/Ebonex catalyst. This is explained with the changes in the binding energy of surface Pt registered by XPS analysis, which is shifted in positive direction relative to Pt/Ebonex with 0.6 eV. The presence of Fe-oxides on the catalyst surface favours the formation of oxygenated surface coverage which, in turn facilitates additionally the OER.

To decrease further the energy consumption, further improvement of the MEA performance is required that can be achieved through optimization of ET30 sintering process to optimize the porosity of GDL. Another approach should be to increase the specific surface of the used non-carbon support.

4. Conclusions

A serias of bimetallic nanosized compositions supported on nonstecheometric Magnelli phase titania are synthesized and investigated as anode catalysts in PEMWE. It isdemonstrated that there is a strong dependence between the electronic density of the metallic components and support and the catalysts structure, morphology, surface properties, and OER efficiency. In PtFe/Ebonex and PtCo/Ebonex both metals form solid solution and realize electronic interactions with the supporting titanium oxide, which results in enhanced OER efficiency. The best performance among all studied catalysts shows PtFe/Ebonex. The water electrolysis efficiency on MEA with PtFe/Ebonex anode exceeds 80%, while the energy consumption for a liter produced hydrogen decreases with about 30% compared to MEA with Pt/Ebonex, having doubled Pt loading. The developed carbon-free gas diffusion electrode is stable at the aggressive conditions of intensive oxygen evolution, while its porosity needs to be further improved to ensure better transport of the reagents and increased catalysts utilization.

Acknowledgements

References

[1] Barbir F. (2005). PEM electrolysi for production of hydrogen from renewable energy sources, *Solar Energy 78*, 661-669

[2] Deschamps A., Etievantb C., Fateev V., Grigoriev S., Klimnikov A., Millet P., Porembski V., Puyenchet C. (2006). Development of advanced PEM water electrolysers, *WHEC 16*, 13-16 june 2006, Lion, France

[3] Ma L., Sui S., Zhai Y. (2009). Invstigaton on high performance proton exchange membrane water electrolyzer, *International Journal of Hydrogen Energy 34*, 678-684.

[4] Matsymoto Y., Sato E. (1986). Electrocatalytic properties of transition metal oxides for oxygen evolution reaction materials, *Chemistry and Physics 14,* 397-426.

[5] Alves V., L. da Silva, Boodts J. (1998). Electrochemical impedance spectroscopic study of dimensionally stable anpde cprrosion, *Journal of Applied Electrochemistry 28* (1998) 899-905

[6] Macpherson J., G. de Mussy J-P., Deplance J-P. (2002). High-resolution electrochemical, electrical, and structural characterization of a dimensionally stable $Ti/TiO_2/Pt$ electrode, *Journal of the Electrochemical Society 149*, B306-B313

[7] Andrievski R. (2003). Review on nanostructured materials, *Journal of Materials Science 38,* 1367-1375

[8]   Jaksic M., Murase K. (2005). Extended Brewer thermodynamic basis of fascilitated thermal hypo-hyper-d-intermetallic phase formation, *CI&CEQ 1*, 156-159

[9]   Neophythidis S., Zaafeiratos S., Papakonstantinou G., Jaksic J., Paloukis F. (2005). Extended Brewer hypo-hyper-d interionicbonding theory: II. Strong metal-support interaction grafting of composite electrocatalysts, *International Journal of Hydrogen Energy 30*, 393-410.

[10]   Jaksic M., Schmickleer W., Botton G. (2012). Advances in Electrocatalysis, *Advances in Physical Chemistry*, rticle ID 1800604, doi: 10.1155/2012/180604

[11]   Bockris J., Otagawa T. (1984). The electrocatalysis of oxygen evolution on peroskites, *Journal of the Electrochemical Society 131*, 2905-2303

[12]   Panizza M., Ouattara L., Baranova E., Comninellis Ch. (2003), DSA-type anode based on conductive porous p-silicon substrate, *Electrochemistry Communications 5*, 365-368.

[13]   Slavcheva E., Nikolova V., Petkova, Lefterova E., Dragieva I., Vitanov T., Budevski E.(2005). Electrocatalytic activity of Pt and PtCo deposited on Ebonex by BH reduction, *Electrochimica Acta 50*, 5444-5448.

[14]   Vicar L., Krastaijic N., Radimilovic V., Jaksic M. (2006). Electrocatalysis by nanoparticles – oxygen reduction on Ebonex/Pt electrode, *Journal of Electroanalytical Chemistry 587,* 99-107

[15]   Mazur P., Polonsky J., Paidar M., Bouzek K. (2012), Non-conductive TiO2 as the anode catatalyst support for PEM water electrolysis, *International Journal of Hydrogen Energy 37*, 12081-12088.

[16]   Kasian O., Luk'yanenko T., Velichenko A., Anadelli R. (2102), Electrochemical behaviour of platinized ebonex electrodes, *International Journal of Hydrogen Energy 7,* 7915-7926.

[17]   Chen G., Bare S., Mallouk T. (2002). Development of supported bifunctional electrocatalysts for unitized regenerative fuel cells, *Journal of The Electrochemical Society 149,* A1092-A1099

[18]   Development of a new material – monolithic Ti_4O_7 Ebonex® Ceramic, http://pubs.rsc.org/doi:10399781847847550699-FX001

[19]   Suntivich J., Gasteiger H., Yabuuchi N., Nakanishi H., Goodenough J., Shao-Horn Y. (2011). Design principles for oxygen-reduction activity on perovskite oxide catalysts for fuel cells and metal–air batteries, *Nature Chemistry 3* (2011), 546–55 0doi:10.1038/nchem.1069

[20]   Stoyanova A., Borisov G., Lefterova E., Slavcheva E. (2012). Oxygen evolution on Ebonex-supported Pt-based binary compounds in PEM water electrolysis, *International Journal of Hydrogen Energy 37,* 16515-16521.

[21]   Lanfgord J., Wilson A. (1978). Survey and some new results in the determination of crystallite size, *Journal of Applied Crystallography 11,* 102-113.

[22]   Borisov G., Stoyanova A., Lefterova E., Slavcheva E. (2013). A novel non-carbon gas diffusion layer for PEM water electrolysis anodes, *Bulgarian Chemical Communications 45,* 186-190.

[23]   Zhang H., Chen L (2010). Preparation and characterization of platinum supported on carbon nanotubes with different tube diameter for cathode catalysts of proton exchange membrane fuel cells, *Journal of Materials Science & Technology 26*, 529-534.

[24]   Vakisaka M., Mitsui S., Hirose Y., Kawashima K., Uchida H., Watanabe M. (2006). Electronic structures of Pt-C0 and Pt-Ru alloys for CO-tolerant anode catalysts in polymer electrolyte fuel cells studied by EC-XPS, *Journal of Physical Chemistry. B 110*, 23489-23496

[25]   Arica A., Shukla A., Kim H., Park S., Min M., Antonucci V. (2001). An XPS study on oxidation states of Pt and its alloys with Co and Cr and its relevance to electrooxidation of oxygen, *Applied Surface Science 172*, 33-40.

[26]   Greeley J., Mavrikakis M. (2005). Surface and subsurface Hydrogen: Adsorption Properties on Transition Metals and Near-surface alloys, *Journal of Physical Chemistry. B 109,* 3460–3471.

[27]   Da Silva L., De Faria L., Boodts J. (2001). Determination of the morphology factor of oxide layers, *Electrochimica Acta 47*, 395-403.